

Biotemplate Synthesis of 3-nm Nickel and Cobalt Nanowires

Mato Knez,[†] Alexander M. Bittner,^{*,†} Fabian Boes,[‡] Christina Wege,[‡] Holger Jeske,[‡] E. Maiß,[§] and Klaus Kern[†]

Max-Planck-Institut für Festkörperforschung, Heisenbergstraße 1, D-70569 Stuttgart, Germany, Universität Stuttgart, Biologisches Institut, Pfaffenwaldring 57, D-70550 Stuttgart, Germany, and Universität Hannover, Institut für Pflanzenkrankheiten und Pflanzenschutz, Herrenhäuser Straße 2, D-30419 Hannover, Germany

Received April 23, 2003; Revised Manuscript Received June 11, 2003

ABSTRACT

Large biomolecules are attractive templates for the synthesis of metal^{1–7} and inorganic^{8–10} compound nanostructures. The well-defined chemical and structural heterogeneity of the biotemplates can be exploited for the precise control of the size and shape of the formed nanostructures. Here, we demonstrate that the central channel of the tobacco mosaic virus (TMV) can be used as a template to synthesize nickel and cobalt nanowires only a few atoms in diameter, with lengths up to the micrometer range.

A key issue in nanotechnology is the development of conceptually simple construction techniques for the mass fabrication of identical nanoscale structures. Conventional “top-down” fabrication techniques are both energy-intensive and wasteful because many production steps involve depositing unstructured layers and then patterning them by removing most of the deposited films. Furthermore, increasingly expensive fabrication facilities are required as the feature size decreases. The natural alternative to top-down construction is the “bottom-up” approach, in which nanoscale structures are built from their atomic and molecular constituents by self-assembly. This approach relies on the exploitation of specific intermolecular interactions and is one of the key building principles of all living organisms. It is thus obvious to search for biological structures that can be used as templates for directing the self-assembly. An ideal biological nano-object for this purpose is the tobacco mosaic virus (TMV), which is a very stable tube-shaped complex of a helical RNA composed of ca. 6400 bases and 2130 identical coat proteins. The rigid virion is 300 nm long, but linear head-to-tail aggregation results in oligomers with lengths of 600, 900 nm, and so forth.¹¹ TMV has an outer diameter of 18 nm; a central channel with a diameter of 4 nm is clad by flexible loops of the protein structure. TMV is thus a perfect molecular nanocylinder. The well-defined chemical groups at specific locations of the coat proteins

can act as ligands for metal ions. We use this chemical functionality for the growth of metal wires from metal ion solutions. TMV is first activated by the selective binding of Pd(II) or Pt(II) ions, followed by metallization with borane-containing nickel and cobalt solutions. Nickel and cobalt wires (3 nm wide) with lengths of up to 600 nm grow selectively in the central channel.

To produce TMV, which is harmless to mammals, we infected *Nicotiana tabacum* cv. Samsun nn plants with plasmid DNA that comprised the code for the movement and coat protein of the TMV genome as well for the replicase. Systemically infected leaves were harvested, and virions were isolated by standard methods. Each virion is composed of the RNA, a helix with an 8-nm diameter, and the coat proteins that are arranged in a helical fashion. The RNA bases fit into pockets in the coat protein structure. Both the outer surface and the channel cladding are hydrophilic, as seen by the presence of water molecules¹² and by the adsorption properties. The outer surface presents mainly hydroxyl groups and the carboxylate terminus of the proteins. (Amine-containing amino acids are present in the groove between two adjacent proteins.) The protein loops in the channel are flexible¹² and can expose various functionalities such as hydroxyl, primary amide, carboxylate, and amine groups.

We explored the extraordinary chemical and physical stability of TMV by treatment with different solvents, by varying pH values, by heating, and by reaction with reducing agents. The analysis was effected by transmission electron microscopy (TEM) with a 200-kV electron beam (Philips

* Corresponding author. E-mail: a.bittner@fkf.mpg.de. Phone: +49 711 689-1433. Fax: +49 711 689-1079.

[†] Max-Planck-Institut für Festkörperforschung.

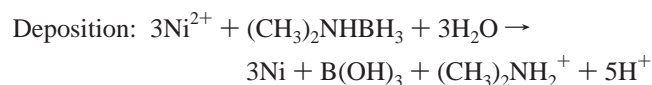
[‡] Universität Stuttgart.

[§] Universität Hannover.

CM200) after the adsorption of the virion on TEM grids or by atomic force microscopy (AFM) in contact and noncontact modes after adsorption on various well-defined surfaces. Temperatures up to 90 °C¹³ and pH values from slightly below the isoelectric point of 3.5 up to about 9 leave the structure largely unaffected for at least several hours.¹⁴ Temperatures up to 80 °C did not change the shape of TMV adsorbed on graphite. The reductants ascorbic acid, hypophosphite, and dimethylamine borane (DMAB) had no effect on the structure.

We observed a certain tendency to form linear virion aggregates, which often reached several micrometers in length (multiples of 300 nm, the length of a single virion).¹¹ These aggregates showed the same adsorption behavior as single virions. Adsorption on oxide-terminated silicon wafers (after NH₃/H₂O₂ and HCl/H₂O₂ treatment) was demonstrated by noncontact AFM measurements (Figure 1a; a ThermoMicroscopes Autoprobe M5 was employed). The height here (*z* direction) was 20% below the expected height of 18 nm, pointing toward deformation due to attractive forces between the virion and substrate. The width (*x* direction) is in the 100-nm range and results from a convolution of the virus shape and the AFM tip shape. On the very hydrophobic graphite surface, TMV had to be adsorbed from a suspension in water/dimethyl sulfoxide, and noncontact AFM was able to image single virions as well as aggregates (Figure 1b) with the expected height of 18 nm.¹⁷ The properties of a TEM grid (coated with evaporated carbon) are located between these two extremes; virions can be adsorbed from suspensions in water.

The stability against pH change, relatively high temperatures, and mild to relatively strong reductants convinced us that the electroless deposition of metals should be possible without virion degradation. Electroless deposition is used industrially to produce metallic coatings with thicknesses in the micrometer range. Nonconductive surfaces undergo activation with Pd(II) and Sn(II), followed by immersion in a deposition bath that comprises metal ions and reductant. The activated surfaces and also the growing metal catalyze the deposition, here shown for the example of pure Pd activation and Ni deposition:



The virions were, after dialysis against pure water, incubated with 0.9 mM PdCl₄²⁻ or PtCl₄²⁻ in 1 M Cl⁻ at pH 5. Under such conditions, the hydrolysis (especially of PdCl₄²⁻) is slow, and only nanoscale oxo-hydroxo compounds (if at all) form,^{15,16} an important prerequisite for limiting the deposition to very small areas. In some cases, dialysis against metal-free chloride solution followed by centrifugation was used to remove metal complexes that were not adsorbed to virions. Dimethylamine borane in water should reduce Pd(II) and Pt(II) to clusters. TEM images (Figure 2b) show increased electron density, compared to

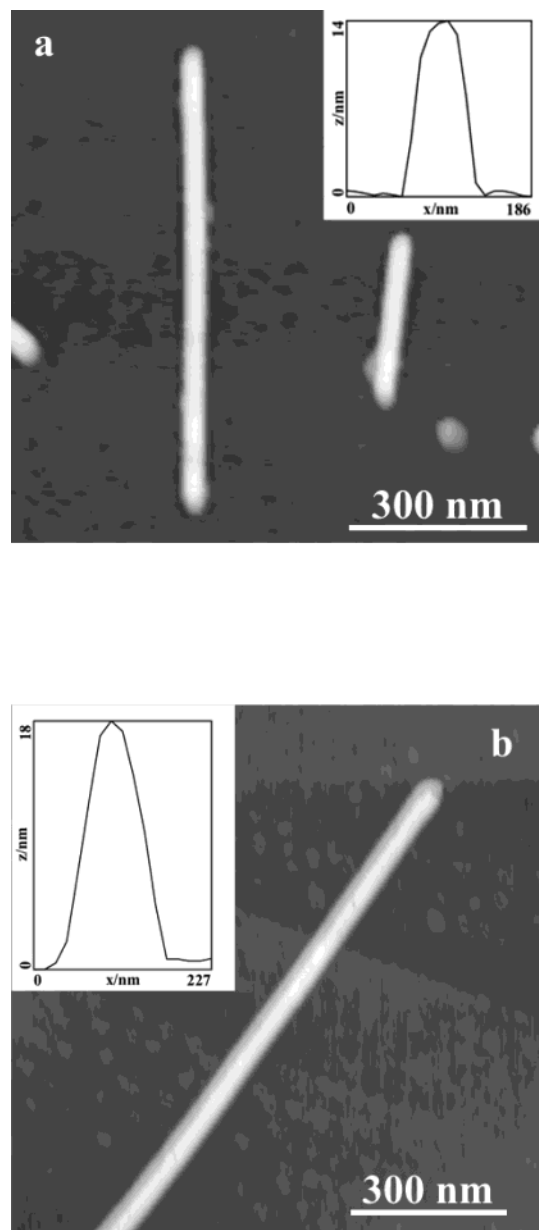


Figure 1. (a) Noncontact AFM image of a linear virion aggregate and a single virion on an oxidized silicon wafer. The profile shows that the height is ca. 14 nm. (b) Noncontact AFM image of a linear virion aggregate on a graphite surface (highly oriented pyrolytic graphite). The profile shows that the height is 18 nm, which corresponds to the diameter.

that shown in images of the pure virion (Figure 2a), hence metallization had occurred. However, we were unable to detect clusters inside the virion, which we ascribe to an activation of the virion with an extremely well dispersed noble metal, presumably in the form of subnanometer clusters. The large aggregates in Figure 2b are Pd clusters arranged on the TEM grid and on the virion coat. The milder reductant hypophosphite gave similar results but, in addition, a dense coverage of the outer virion surface with clusters of >4 nm diameter (results not shown). Their absence after further processing indicates that they are only loosely bound to the virion and easily removed.

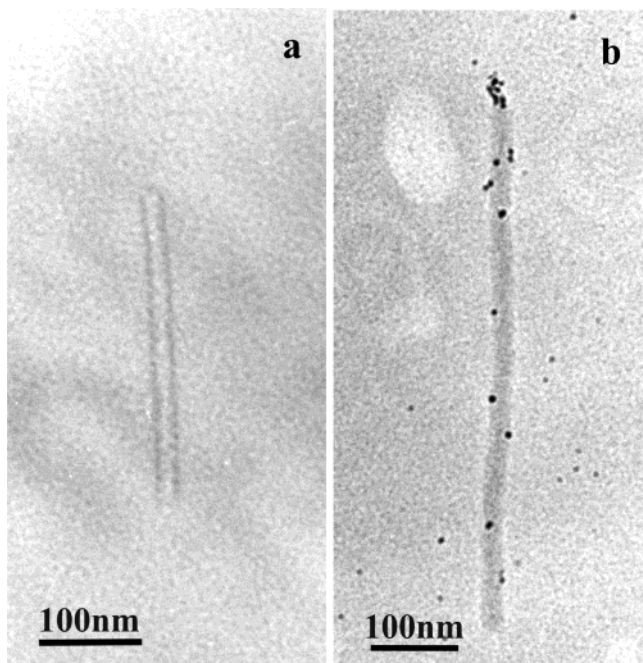


Figure 2. (a) TEM image of a TMV particle. Only the contours appear dark; the coat proteins and the central channel are transparent. The sample was not stained. (b) TEM image of TMV after Pd(II) adsorption (“activation”), followed by reduction. The virion appears much darker than in panel a. Some clusters are adsorbed on the outer surface; several more without contact to TMV can be found on the TEM grid.

After activation with Pd(II) and Pt(II) as detailed above, virions were dispersed in electroless deposition baths of pH 6–8 at 25 °C. The baths contained a reductant and either Co(II) or Ni(II). After 3 min, samples were removed from the bath, transferred to TEM grids, dried quickly, and analyzed. Whereas hypophosphite baths resulted in spherical clusters of 3-nm diameter in the central channel⁵ and only in some cases in elongated clusters of several tens of nanometers in length (other methods yield metal clusters of ca. 5-nm diameter⁶), dimethylamine borane baths produced continuous nanowires of about 3-nm diameter (Figure 3a and b) in ca. 30% of all virions. The exact diameter of the nanowire was difficult to measure because the borders of the wire were not always clearly visible. In addition, some optical error (<1 nm) due to photographic processing is possible. In linear TMV aggregates, the straight wires reached lengths of more than 500 nm without gaps, which means that wires can bridge two virions. This is direct proof that linear TMV aggregates have a single uninterrupted central channel. We found no difference in employing Pt or Pd for the activation, but without activation, metallization was impossible.

Clearly, the growth of wires, as opposed to clusters, depends critically on the activation of the biomolecule and on the proper choice of reductant. Wires have to grow inside the channel, so the metal ions, Pd(II) and Pt(II) complexes, have to reach the central channel, but preformed clusters with diameters >4 nm are unable to enter. PdCl₄²⁻ and PtCl₄²⁻ should be unable to bind electrostatically to the negatively charged channel⁶ but may also form complexes with amine

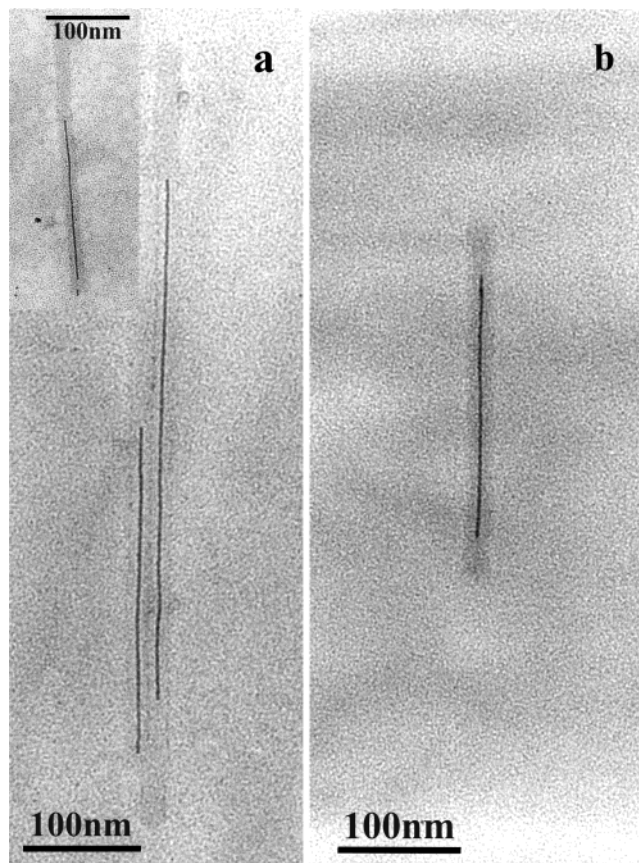


Figure 3. (a) TEM image of TMV after Pd(II) activation, followed by electroless deposition of Ni. Two adjacent virion aggregates are filled with wires; the left aggregate comprises three TMV particles whose combined channels are filled to a length of 600 nm. Energy-resolved scanning TEM images proved that the dark wire is indeed composed of Ni. Inset: A single virion is filled with a 200-nm-long wire with a ca. 3-nm diameter. (b) TEM image of TMV after Pd(II) activation, followed by electroless deposition of Co. The virion is filled by a 200 nm-long wire with a ca. 3-nm diameter.

groups,⁵ a process with surprisingly little dependence on pH values.¹⁵ The outer TMV surface of our virus strain (*vulgare* with Ser-155 replacing Gly-155) does not offer amines, hence the spatial selectivity for the channel. Note that electroless deposition with mild reductants appears to stop after a certain cluster size (on the order of nanometers) is reached. Concurrence with the reduction of dissolved oxygen and nanoscopic transport phenomena close to a growing cluster is responsible for this behavior.¹⁵ Further deposition requires more aggressive reductants and is based on the surprising fact that TMV is not significantly altered by strong reductants, yet another proof of its extraordinary resilience. The finely dispersed activation centers (Pd or Pt clusters) support the synchronous growth of each center. Coalescence of the growing nuclei inside the channel finally results in the wire shape without gaps in the metal structure.

A scale-up of our procedure should be possible; for the electroless deposition bath especially, the usual precautions should be taken (i.e., control of pH and temperature, convection, and continuous filtration to remove metal particles larger than a few micrometers). The limits would then be the centrifugation of large volumes and the avail-

ability of virus material (20 plants yield 1 g of TMV, corresponding to a 4.5×10^9 m tube length). The importance of producing wires in the way we present here is not only that their diameter is extremely small and that their aspect ratio is very high. In addition, the presence of the virion around the wire opens up numerous further perspectives. For example, biochemical and microbiological techniques can produce chemically modified virions and mutations in the coat protein. This will allow for the planning of the synthesis of a variety of shapes and sizes of metal wires, in sharp contrast to today's "trial and error" strategies. In addition, the wires can be placed with exact control on a substrate, relying on chemical interactions between the virion and substrate.¹⁷ Contacting the wire should be possible not only in top-down fashion by standard lithography but also in bottom-up fashion by tagging with antibodies whose chemical code would recognize targets; altering amino acids should also allow for the binding of metal ions very tightly on the outer surface, thus permitting homogeneous metallization to form cylinders. The TMV template allows for the complete bottom-up synthesis and placement of a nanowire: formation of a wire or a cylinder at a virion, binding of the modified virion by chemical coding to a specified target (e.g., a small area on a solid substrate) and thereafter the induction of the disassembly of proteins and RNA (e.g., at high pH or enzymatically), and recycling of the biomolecules.

Acknowledgment. We thank M. Kelsch and Dr. F. Phillipp (MPI für Metallforschung, Stuttgart) for help with

the TEM measurements and C. Kocher (Universität Stuttgart) for technical assistance.

References

- (1) Mertig, M.; Wahl, R.; Lehmann, M.; Simon, P.; Pompe, W. *Eur. Phys. J. D* **2001**, *16*, 317.
- (2) Richter, J.; Mertig, M.; Pompe, W.; Mönch, I.; Schackert, H. K. *Appl. Phys. Lett.* **2001**, *78*, 536. Mertig, M.; Ciacchi, L. C.; Seidel, R.; Pompe, W. *Nano Lett.* **2002**, *2*, 841.
- (3) Mertig, M.; Kirsch, R.; Pompe, W. *Appl. Phys. A* **1998**, *66*, S723.
- (4) Braun, E.; Eichen, Y.; Sivan, U.; Ben-Yoseph, G. *Nature* **1998**, *391*, 775.
- (5) Knez, M.; Sumser, M.; Bittner, A. M.; Wege, C.; Jeske, H.; Kooi, S.; Burghard, M.; Kern, K. *J. Electroanal. Chem.* **2002**, *522*, 70.
- (6) Dujardin, E.; Peet, C.; Stubbs, G.; Culver, J. N.; Mann, S. *Nano Lett.* **2003**, *3*, 413.
- (7) Wang, Q.; Lin, T.; Tang, L.; Johnson, J. E.; Finn, M. G. *Angew. Chem., Int. Ed.* **2002**, *41*, 459.
- (8) Shenton, W.; Pum, D.; Sleytr, U. B.; Mann, S. *Nature* **1997**, *389*, 585.
- (9) Lee, S.-W.; Mao, C.; Flynn, C. E.; Belcher, A. M. *Science* **2002**, *296*, 892.
- (10) Douglas, T.; Young, M. *Nature* **1998**, *393*, 152.
- (11) Falvo, M. R.; Washburn, R.; Superfine, R.; Finch, M.; Brooks, F. P., Jr.; Chi, V.; Taylor, R. M., II. *Biophys. J.* **1997**, *72*, 1396.
- (12) Bhyravbhata, B.; Watowich, S. J.; Caspar, D. L. D. *Biophys. J.* **1998**, *74*, 604.
- (13) Zaitlin, M. *AAB Descriptions of Plant Viruses* **2000**, *370*, 8.
- (14) Perham, R. N.; Wilson, T. M. A. *Virology* **1978**, *84*, 293.
- (15) Kind, H.; Bittner, A. M.; Cavalleri, O.; Kern, K.; Greber, T. *J. Phys. Chem. B* **1998**, *102*, 7582.
- (16) Bittner, A. M.; Wu, X. C.; Kern, K. *Adv. Funct. Mater.* **2002**, *12*, 432.
- (17) Knez, M.; Sumser, M. P.; Bittner, A. M.; Wege, C.; Jeske, H.; Hoffmann, D. M. P.; Kuhnke, K.; Kern, K., submitted for publication.

NL0342545